

# Tailored quantum dots for entangled photon pair creation

A. Grelich, M. Schwab, T. Berstermann, T. Auer, R. Oulton, D. R. Yakovlev, and M. Bayer  
*Experimentelle Physik II, Universität Dortmund, D-44221 Dortmund, Germany*

V. Stavarache, D. Reuter, and A. Wieck  
*Angewandte Festkörperphysik, Ruhr-Universität Bochum, D-44780 Bochum, Germany*  
 (Dated: December 17, 2017)

We compare the asymmetry-induced exchange splitting  $\delta_1$  of the bright-exciton ground-state doublet in self-assembled (In,Ga)As/GaAs quantum dots, determined by Faraday rotation, with its homogeneous linewidth  $\gamma$ , obtained from the radiative decay in time-resolved photoluminescence. Post-growth thermal annealing of the dot structures leads to a considerable increase of the homogeneous linewidth, while a strong reduction of the exchange splitting is simultaneously observed. The annealing can be tailored such that  $\delta_1$  and  $\gamma$  become comparable, whereupon the carriers are still well confined. This opens the possibility to observe polarization entangled photon pairs through the biexciton decay cascade.

PACS numbers: 71.36.+c, 73.20.Dx, 78.47.+p, 42.65.-k

Entangled photon pairs are a key requirement for the implementation of quantum teleportation schemes. [1] Typically, such photon pairs are created by parametric down conversion of a strongly attenuated laser beam in a non-linear optical crystal, with limited efficiency. Recently, the decay of a biexciton complex confined in a quantum dot (QD) has been suggested as an efficient source for polarization entangled photon pairs. [2] This concept was based on the assumption of an idealistic QD structure for which the valence band ground state has pure heavy hole character with angular momentum projections  $J_{h,z} = \pm 3/2$  along the heterostructure growth direction. When an electron-hole pair is injected, the momenta of the carriers become coupled by the exchange interaction. If the dot has perfect  $D_{2d}$ -symmetry, angular momentum is a good quantum number: the optically active states with momenta  $M = \pm 1$  are degenerate, and their decay leads to emission of  $\sigma^\pm$ -circularly polarized photons.

If the dot ground states are occupied by two electrons and two holes, each with opposite spin orientations, a spin singlet biexciton  $X_2$  is formed, for whose decay two channels exist, as shown in Fig. 1 (upper panel left). The first photon is emitted with either  $\sigma^+$  or  $\sigma^-$ -polarization, and then the second photon with opposite polarization, as long as no spin flip occurs after the first process. Unless a polarization measurement is performed, the two photon polarization state is therefore described by  $|2\gamma\rangle = (|+\rangle_1 |-\rangle_2 + |-\rangle_1 |+\rangle_2) / \sqrt{2}$ , forming an entangled state. A key requirement is that the photons emitted at each stage of the cascade are quasi-degenerate within their homogeneous linewidth, such that they cannot be distinguished by an energy measurement.

Experiments have failed up to now to demonstrate such an entanglement, as only classical correlations were observed. [3] While some of the idealizations of the original proposal are well fulfilled, for example, for strongly confined self-assembled (In,Ga)As/GaAs quantum dots (such as the long exciton spin relaxation time as com-

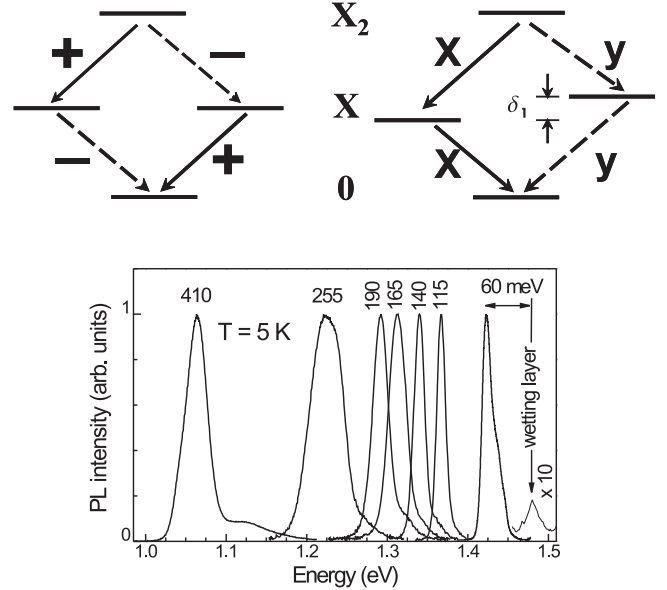


FIG. 1: Upper: Scheme of the possible decay channels of a biexciton  $X_2$  confined in a QD. Left hand side gives the situation for an idealized dot with  $D_{2d}$ -symmetry, while the right hand side does the same for a dot with reduced symmetry. Plus/minus signs and x/y signs indicate circular and linear polarization of the emitted photons, respectively. Lower: Low excitation photoluminescence spectra of QD ensembles annealed at different temperatures, leading to different confinement potentials, as indicated at each spectrum.

pared to the radiative lifetime [4], or the almost pure heavy-hole character of the valence band ground state [6]), a fundamental problem arises from the broken  $D_{2d}$  symmetry, which is reduced to at least  $C_{2v}$  or even lower symmetry in realistic dot structures. [7, 8, 9] As a consequence, angular momentum is no longer a good quantum

number and the  $\pm 1$  excitons become mixed to linearly polarized eigenstates, resulting in an energy splitting  $\delta_1$  of the bright exciton doublet (see Fig. 1, upper panel right). Generally, this splitting is considerably larger than the homogeneous linewidth of the exciton. Therefore the two decay channels can be distinguished even without a polarization measurement, simply by measuring the energy of the first photon. Photon entanglement is not preserved in this case.

The only way to achieve polarization entanglement is to reduce the splitting such that  $\delta_1$  becomes smaller than the homogeneous linewidth  $\gamma$ , which at cryogenic temperatures is radiatively limited. [10] Several strategies have been pursued to reach the goal of a quasi-degeneracy of the bright exciton doublet. One example is the application of an electric field in the quantum dot plane, to compensate the asymmetry. This has shown some promise, but the reduction of  $\delta_1$  was still too small. [11] Lately, it was found by non-linear optical techniques that thermal annealing may lead to a strong reduction of the exchange splitting down to the few  $\mu\text{eV}$ -range. [12, 13] Very recently, it has been demonstrated by single dot spectroscopy that, within the experimental accuracy, the splitting may even become zero or its sign may be reversed. [14]

Here we complete this picture by addressing not only the asymmetry splitting for dots with varying confinement, but we also compare this splitting to the homogeneous linewidth  $\gamma$ : Any reduction of  $\delta_1$  even to very small values would not enable entanglement as long as  $\delta_1 > \gamma$ . We show that the two energies may be made comparable through an annealing step, which, however, still keeps the dot carriers well confined. For determining the energies we use spectroscopic techniques complementary to those used previously, and we compare the results to data reported in literature.

The experiments were performed on arrays of self-assembled (In,Ga)As/GaAs QDs. To obtain strong enough light-matter interaction, the samples contained 20 layers of QDs, that were separated by 60 nm wide barriers. The structures were fabricated by molecular beam epitaxy on (001)-oriented GaAs substrate. The samples were annealed for 30 s at different temperatures  $T_{ann}$  between 800 and 980°C by which the confinement is reduced due to intermixing between dot and barrier material. Fig. 1 (lower panel) shows typical photoluminescence spectra of samples differing in  $T_{ann}$ , which show the established behavior for such a series of structures: [5] With increasing  $T_{ann}$ , a blue shift as well as a narrowing of the emission line is observed. Even though there is a clear trend of increasing emission energy with increasing  $T_{ann}$  for the samples under study, an exact correlation cannot be made. As a more characteristic quantity for the electronic confinement therefore we in the following label the samples by the confinement potential, which we define as energy separation of the ground state dot emission from the wetting layer at about 1.48 eV. The wetting layer emission also shifts to higher energies with

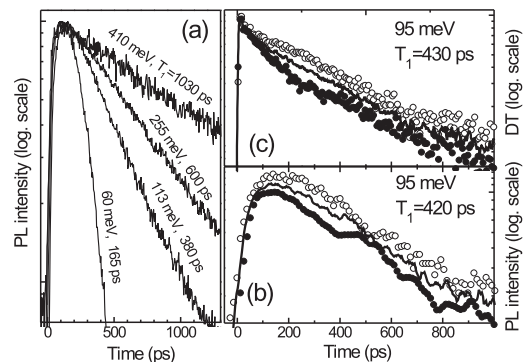


FIG. 2: (a) Time-resolved photoluminescence of QD ensembles with different confinement without polarization analysis. Excitation power was  $1 \text{ W cm}^{-2}$ . (b) Same as (a), but for a sample with 95 meV confinement. Excitation into wetting layer was  $\sigma^+$ -polarized, detection was either  $\sigma^+$  (open circles) or  $\sigma^-$ -polarized (solid circles). Solid line gives average of both traces. (c) Differential transmission for same sample as in panel (b). Pump beam was  $\sigma^+$ -polarized, probe either  $\sigma^+$  (open circles) or  $\sigma^-$ -polarized (solid circles). Solid line again gives average.

increasing  $T_{ann}$ , but this shift is weak. The confinement energies range from 410 down to 60 meV.

The samples were immersed in helium gas at a temperature of 5 K. Optical excitation was done by a mode-locked Ti-sapphire laser emitting pulses with a duration of about 1 ps at 75.6 MHz repetition rate, which hit the sample along the heterostructure growth direction.

The exciton lifetimes were studied using time-resolved photoluminescence, for which the wavelength of the pulsed laser was tuned to the GaAs band gap at 1.512 eV. The emission was dispersed by a 0.5 m monochromator and detected by a streak camera with a S1 photocathode. Excitation powers as low as possible were used to study the pure exciton decay by avoiding multiparticle occupation effects such as Pauli blocking and related ground shell refilling. Fig. 2(a) shows decay curves of four different QD samples. The excitation was linearly polarized, while the emission was detected without polarization resolution. One clearly sees that the decay is the faster, the shallower the confinement is. The observed decays have been analyzed by single exponential fit, and the decay times are indicated at each trace. The decay time decreases from 1030 to 165 ps with decreasing confinement. This behavior is expected: the exciton lifetime is determined by the exciton coherence volume, which is given by the dot size. The size is increased by the annealing step, leading to the decrease of the exciton lifetime.

Fig. 2(b) shows time-resolved PL spectra of a sample with a confinement potential of 95 meV. In this case the

excitation was  $\sigma^+$ -circularly polarized and resonant with the wetting layer at about 1.48 eV. Detection was taken either  $\sigma^+$  (open circles) or  $\sigma^-$  (solid circles) polarized. For clarity, the two curves have been shifted vertically relative to each other. The average of these traces is also shown (the solid line) which follows to a good approximation an exponential dependence with a decay time of 420 ps. The polarization-resolved decays show some modulation which is in antiphase for the two curves. A rough estimate gives a period of  $600 \pm 50$  ps for the oscillation, which corresponds to an energy splitting of about  $7 \mu\text{eV}$ . This is comparable to the expected fine structure splitting  $\delta_1$ . [12]

A priori it is not clear that time-resolved PL measurements yield the exciton lifetime  $T_1$ , in particular for non-resonant excitation, as the dynamics involves also carrier relaxation. Therefore we have also performed pump-probe differential transmission studies on the 95 meV confinement sample: The pump beam was resonant to the ground state dots transition and excites a corresponding carrier population, whose decay is then tested by a probe beam. The data are shown in Fig. 2(c). The traces show data with  $\sigma^+$  pump excitation, and  $\sigma^+$  (open circles) and  $\sigma^-$  (solid circles) -polarized detection, respectively. The solid line gives again the average of the two traces, resulting in a decay time of 430 ps. Within the experimental error, this time agrees well with that obtained by time-resolved photoluminescence, confirming that under the applied experimental conditions, the PL decay time does indeed give the exciton lifetime  $T_1$ , from which the homogeneous linewidth  $\gamma = 2\hbar/T_1$  is obtained (see Fig. 4). Note that for the polarized differential transmission traces an antiphase modulation is again observed, even though it is too weak to determine an oscillation period.

As mentioned, studies of the exchange interaction induced splitting have been up to now reported by photoluminescence on single QDs [7, 8] or by non-linear spectroscopy such as four-wave-mixing [12] or differential transmission [13] on ensembles. Here we use another non-linear technique to address this problem, namely pump-probe Faraday rotation [15], for which the laser was tuned to the energy of the ground state transition in the QDs and split into two trains: An electron spin polarization is induced by a circularly polarized pump beam and is tested by the rotation of the linear polarization of a probe beam. For recording the rotation angle, a homodyne technique based on phase-sensitive balanced detection was used.

Following previous results for small  $\delta_1$  values [12], we focused in these experiments on strongly annealed dots with small confinement potentials. Fig. 3(a) shows Faraday rotation signals for two samples with confinement potentials of 140 and 95 meV. The polarization direction of the probe beam was directed along the [100] crystal axis. Strongly damped oscillations are observed in both cases (note that the data were recorded at zero magnetic field), as a result of precession of the exciton

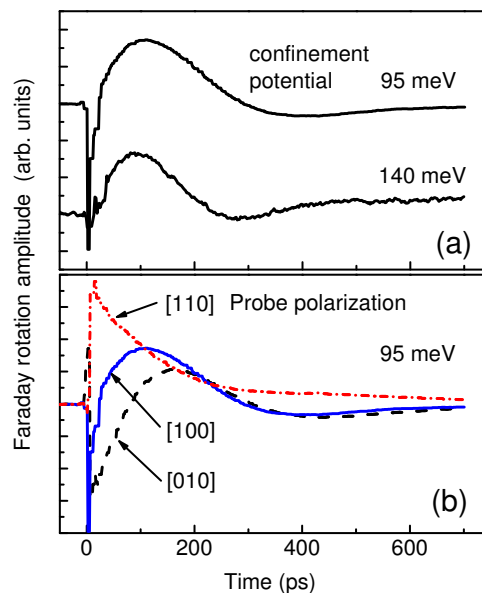


FIG. 3: (a) Faraday rotation signal with probe beam polarized linearly along the [100] crystal direction for samples with confinement potentials of 95 and 140 meV. (b) Faraday rotation traces recorded on the sample with 95 meV confinement potential for different linear polarization orientations of probe beam. In both cases, the pump beam was  $\sigma^+$ -polarized.  $T = 5$  K.

angular momentum about the in-plane anisotropy axes of the QDs along [110] and  $[1\bar{1}0]$ . This precession reflects the quantum beats occurring due to the coherent excitation of both linearly polarized exciton eigenstates  $|\Psi_{1,2}\rangle \propto | +1\rangle \pm | -1\rangle$  by the circularly polarized pump pulse. The data can be analyzed by an oscillatory fit function with an exponentially damped amplitude. The oscillation period is clearly shorter for the sample with a stronger confinement potential (390 ps) as compared to the sample with weaker confinement (600 ps). The energy splittings  $\delta_1$  that are derived from the oscillation period are 10.5 and  $7.1 \mu\text{eV}$  for the 140 and 95 meV samples, respectively. These values agree very well with data determined from four-wave-mixing on samples with comparable confinement. [12]

For clarity we note that in the pump-probe measurements true quantum beats are observed due to direct resonant excitation of the exchange-split ground state exciton, while in the time-resolved photoluminescence studies with non-resonant excitation described above the observed oscillation are due to polarization interferences of the emitted photons. [16]

For understanding the observed Faraday rotation more intuitively, a pseudospin formalism can be used for the exciton description. [17] The bright exciton doublet with  $|M| = 1$  is described by the matrix

$$\mathcal{H} = \begin{pmatrix} E_0 + \frac{\delta_0}{2} & \frac{\delta_1}{2} \\ \frac{\delta_1}{2} & E_0 + \frac{\delta_0}{2} \end{pmatrix},$$

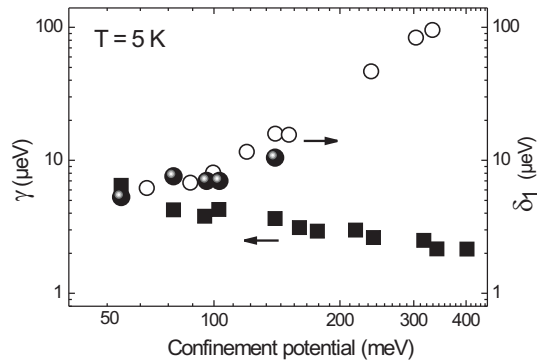


FIG. 4: Homogeneous linewidth  $\gamma$  (squares) and exchange splitting  $\delta_1$  (circles) of the exciton in InGaAs/GaAs quantum dots as function of the confinement potential. Solid circles are measured with Faraday rotation; open circles are taken from Ref. [12]. Squares are measured by time resolved PL.

where  $E_0$  is the exciton energy, disregarding exchange interaction effects, and  $\delta_0$  gives the energy splitting between the bright excitons with  $|M| = 1$  and the dark excitons with  $|M| = 2$ . This Hamiltonian can be rewritten as  $\mathcal{H} = (E_0 + \delta_0/2)I + \delta_1\sigma_x/2$ , where  $I$  is the identity and  $\sigma_x$  is the Pauli matrix. The second term has the same form as that of a spin in a perpendicular magnetic field pointing along the  $x$ -direction, resulting in the observed precession.

Fig. 3(b) shows different Faraday rotation traces of the QD sample with 95 meV confinement. The polarization direction of the probe beam, as indicated by the corresponding crystal directions, was varied. The probe polarization has no influence on the beat period, but evidently affects the phase of the oscillation. The exciton state created by the circularly polarized light is given by the superposition state

$$\Psi \propto \Psi_1 \exp\left(-i\frac{\delta_1 t}{2\hbar}\right) + \Psi_2 \exp\left(+i\frac{\delta_1 t}{2\hbar}\right). \quad (1)$$

At a certain time, different components of this state are tested by varying the polarization of the probe, causing the phase shift of the Faraday rotation. In particular, a  $\pi$ -phase shift occurs for a  $90^\circ$ -deg. rotation of the probe polarization from [010] to [110].

Fig. 4 gives an overview of  $\gamma$  and  $\delta_1$  as function of the confinement potential. Note that both values are plotted on a logarithmic scale, as is the confinement potential. The solid circles and solid squares give the exchange splitting and homogeneous linewidth, respectively, measured in our experiments. For comparison, the open circles give the  $\delta_1$  values from Ref. [12]. For the as-grown QD sample with the highest confinement,  $\delta_1$  is by a factor 50 larger than the homogeneous linewidth. This holds for all samples with confinement potentials larger than about 300 meV. Most studies reported up to now on polarization entangled photons were done on comparable structures. The data in Fig. 4 underlines why no entanglement was observed yet.

However, when the confinement potential height is decreased to less than 300 meV, a drastic reduction of the exchange splitting is observed. Simultaneously, the homogeneous linewidth increases. For the QDs with confinement potential around 100 meV, both quantities are of comparable magnitude. For the most shallow QDs,  $\delta_1$  is reduced down to about 5  $\mu\text{eV}$ , while  $\gamma$  is increased to 7  $\mu\text{eV}$ . For these QDs the exchange splitting can no longer be resolved by an energy measurement. It is these QDs from which polarization entangled photon pairs might be expected, and which we will study in the future. For this purpose the cross-correlation should be measured for the biexciton decay cascade in a single QD by a Hanbury-Brown-Twiss setup. [3]

In summary, we have demonstrated that thermal annealing performed on QDs favors a situation in which polarization entangled photon pairs may be observed. On one hand, it reduces strongly the asymmetry-induced exchange splitting of excitons. On the other hand, it simultaneously increases the exciton homogeneous linewidth, under which a finite splitting may be hidden. The latter effect may be enhanced further if the QDs were placed in an optical resonator, which could be used not only for reducing the exciton lifetime through the Purcell effect [18], but also for funnelling the emission into a desired spatial direction, thus enhancing the collection efficiency. [18, 19, 20]

**Acknowledgements.** We are grateful to E.L. Ivchenko for insightful discussions. The work was supported by the DFG (research group 'Quantum Optics of Semiconductor Heterostructures'). R. O. thanks the Alexander von Humboldt foundation.

- 
- [1] D. Bouwmeester, A. Ekert, and A. Zeilinger, *The Physics of Quantum Information*, Springer, Berlin (2000).  
 [2] O. Benson, C. Santori, M. Pelton, Y. Yamamoto, Phys. Rev. Lett. **84**, 2513 (2000).  
 [3] see, for example, E. Moreau, I. Robert, L. Manin, V. Thierry-Mieg, J. M. Gerard, I. Abram, Phys. Rev. Lett. **87**, 183601 (2001); C. Santori, D. Fattal, M. Pelton,

- G. S. Solomon, Y. Yamamoto, Phys. Rev. B **66**, 45308 (2002); R. M. Stevenson, R. M. Thompson, A. J. Shields, I. Farrer, B. E. Kardynal, D. A. Ritchie, M. Pepper, Phys. Rev. B **66**, 081302(R) (2002).  
 [4] M. Paillard, X. Marie, P. Renucci, T. Amand, A. Jbeli, and J. M. Gerard, Phys. Rev. Lett. **86**, 1634 (2001).  
 [5] see, for example, S. Fafard and C. Allen, Appl. Phys.

- Lett. **75**, 2374 (1999).
- [6] see, for example, S. Cortez, O. Krebs, P. Voisin, and J. M. Gerard, Phys. Rev. B **63**, 233306 (2001).
- [7] M. Bayer, A. Kuther, A. Forchel, A. Gorbunov, V. B. Timofeev, F. Schfer, J. P. Reithmaier, T. L. Reinecke and S. N. Walck, Phys. Rev. Lett. **82**, 1748 (1999).
- [8] see, for example, M. Bayer, G. Ortner, O. Stern, A. Kuther, A. A. Gorbunov, A. Forchel, P. Hawrylak, S. Fafard, K. Hinzer, T. L. Reinecke, S. N. Walck, J. P. Reithmaier, F. Klopff, and F. Schfer, Phys. Rev. B **65**, 195315 (2002) and references therein.
- [9] see, for example, G. Bester and A. Zunger, Phys. Rev. B **71**, 045318 (2005).
- [10] W. Langbein, P. Borri, U. Woggon, V. Stavarache, D. Reuter, and A. D. Wieck, Phys. Rev. B **70**, 033301 (2004).
- [11] K. Kowalik, O. Krebs, A. Lematre, S. Laurent, P. Senellart, P. Voisin, and J. A. Gaj, Appl. Phys. Lett. **86**, 041907 (2005).
- [12] W. Langbein, P. Borri, U. Woggon, V. Stavarache, D. Reuter, A. D. Wieck, Phys. Rev. B **69**, 161301(R) (2004).
- [13] A. I. Tartakovskii, M. N. Makhonin, I. R. Sellers, J. Cahill, A. D. Andreev, D. M. Whittaker, J-P. R. Wells, A. M. Fox, D. J. Mowbray, M. S. Skolnick, K. M. Groom, M. J. Steer, H. Y. Liu, and M. Hopkinson, Phys. Rev. B **70**, 193303 (2004).
- [14] R. J. Young, R. M. Stevenson, A. J. Shields, P. Atkinson, K. Cooper, D. A. Ritchie, K. M. Groom, A. I. Tartakovskii, and M. S. Skolnick, Phys. Rev. B **72**, 113305 (2005).
- [15] D. D. Awschalom and N. Samarth, in *Semiconductor Spintronics and Quantum Computation*, edited by D. D. Awschalom, D. Loss, and N. Samarth, Springer Berlin (2002).
- [16] For a detailed discussion see, for example, M. Sns, B. Urbaszek, X. Marie, T. Amand, J. Tribollet, F. Bernardot, C. Testelin, M. Chamarro, and J.-M. Grard, Phys. Rev. B **71**, 115334 (2005), and references therein.
- [17] E.L. Ivchenko, *Optical Spectroscopy of semiconductor nanostructures*, Alpha Science International, Harrow (2005).
- [18] E.M. Purcell, Phys. Rev. **69**, 681 (1946).
- [19] J. M. Grard, B. Sermage, B. Gayral, B. Legrand, E. Costard, and V. Thierry-Mieg, Phys. Rev. Lett. **81**, 1110 (1998).
- [20] B. Ohnesorge, M. Bayer, A. Forchel, J. P. Reithmaier, N. A. Gippius, and S. G. Tikhodeev, Phys. Rev. B **56**, R4367 (1997).